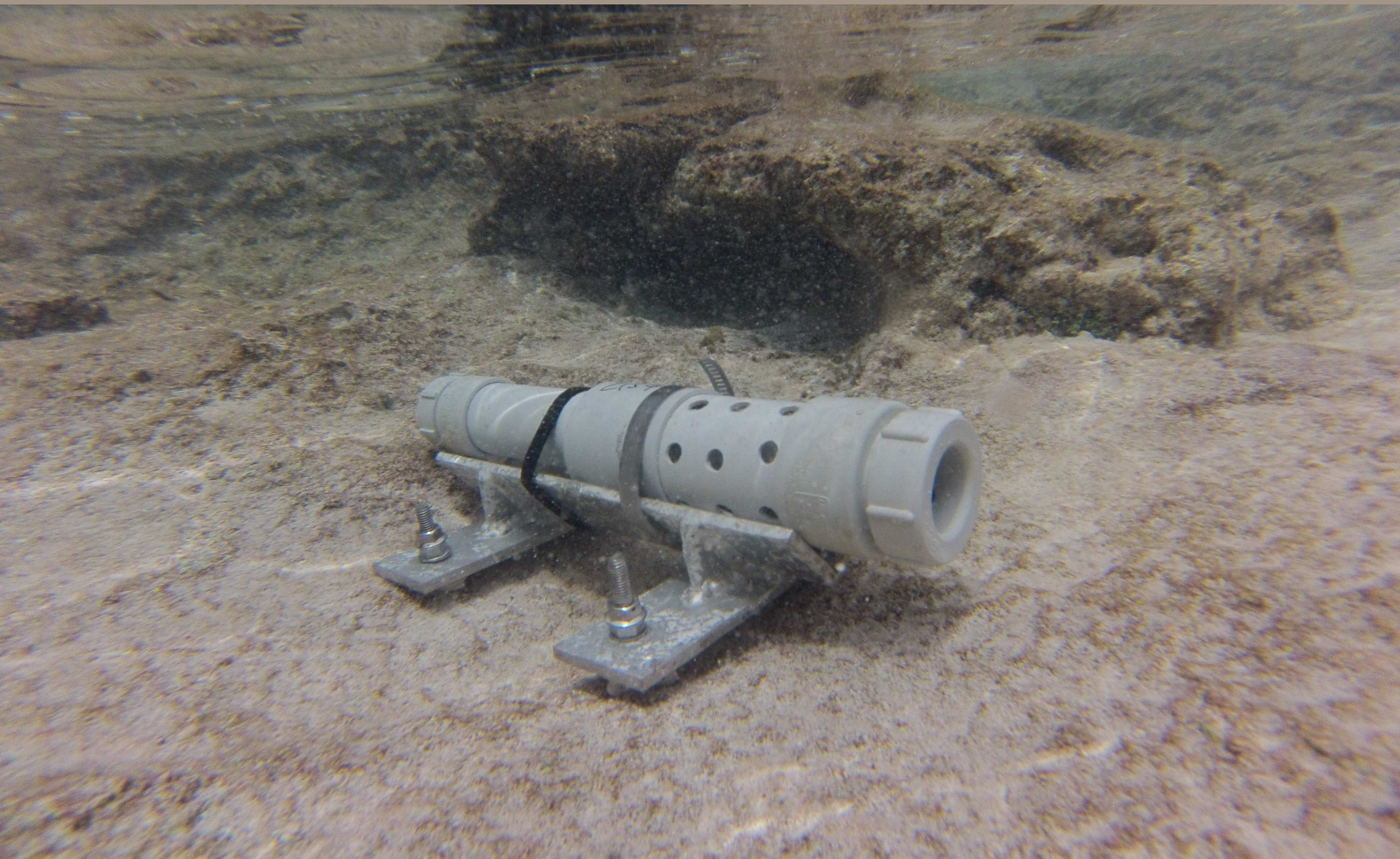


Waves and Coasts in the Pacific

Fatato (Tuvalu), Oceanographic,
Topographic Data Collection



Cyprien Bosserelle, Deepika Lal, Make Movono, Zulfikar Begg,
Salesh Kumar, Sandeep Reddy Eddie Beetham,
Susanne Pohler, Paul Kench, Jens Krüger



Pacific
Community
Communauté
du Pacifique



UNESCO-IHE
Institute for Water Education



Waves and Coasts in the Pacific (WACOP)

Fatato (Tuvalu), Oceanographic, Topographic data
collection

Cyprien Bosserelle, Deepika Lal, , Make Movono,
Zulfikar Begg, Salesh Kumar, Sandeep Reddy , Eddie Beetham, Susanne Pohler, Paul Kench,
Jens Krüger



www.gsd.spc.int/wacop/

© Pacific Community (SPC) 2016

All rights for commercial / for profit reproduction or translation, in any form, reserved. SPC authorises the partial reproduction or translation of this material for scientific, educational or research purposes, provided that SPC and the source document are properly acknowledged. Permission to reproduce the document and/or translate in whole, in any form, whether for commercial / for profit or non-profit purposes, must be requested in writing. Original SPC artwork may not be altered or separately published without permission.

Original text: English

SPC technical Report SPC00045

July 2016

This research was conducted as part of the Waves and Coasts in the Pacific project (WACOP project), financed by the European Union, Grant Number FED/2011/281-131.

DISCLAIMER

While care has been taken in the collection, analysis, and compilation of the data, they are supplied on the condition that the Pacific Community shall not be liable for any loss or injury whatsoever arising from the use of the data.

The contents of this publication are the sole responsibility of the Pacific Community and can in no way be taken to reflect the views of the European Union or other partners of the WACOP project.

Pacific Community
Geoscience Division (GSD)
Private Mail Bag, GPO Suva, Fiji Islands
Telephone: (679) 338 1377
Fax: (679) 337 0040
Email: cyprienb@spc.int
www.spc.int
www.gsd.spc.int/wacop/

Contents

| | |
|--|----|
| Acknowledgements | 4 |
| Executive summary | 5 |
| 1 Background | 6 |
| 1.1 Aims of the WACOP project | 6 |
| 1.2 This report..... | 6 |
| 2 Site Overview | 7 |
| 2.1 Morphology and Geology | 8 |
| 2.1.1 Geography..... | 8 |
| 2.1.2 Reef flat morphology | 9 |
| 2.1.3 Beach morphology | 10 |
| 3 Oceanography | 11 |
| 3.1 Deployments..... | 11 |
| 3.2 Oceanographic data Post processing..... | 13 |
| 3.2.1 Waves..... | 13 |
| 3.2.2 Water levels | 17 |
| 3.2.3 Currents..... | 19 |
| 3.2.4 Tide..... | 20 |
| 4 Topography | 21 |
| 4.1 Benchmarks..... | 21 |
| 4.2 Beach Profile | 22 |
| 4.3 PPK topography..... | 28 |
| 5 Shoreline | 29 |
| 6 Discussion :Fatato Morphodynamics from month, years and decades..... | 30 |
| 7 Conclusion..... | 31 |
| 8 Data download and Citation | 31 |
| 9 Reference | 32 |

Acknowledgements

This work is part of the Waves and Coasts in the Pacific (WACOP) project, which is implemented by the Pacific Community (SPC) in collaboration with the University of the South Pacific, UNESCO-IHE, the Commonwealth Scientific and Industrial Research Organisation, and the University of Auckland. This project is funded under the ACP Caribbean & Pacific Research Programme for Sustainable Development, a programme funded by the European Union (EU) and implemented by the African, Caribbean and Pacific Group of States (ACP Group).

The field work was only possible with the continued support of the Tuvalu Government and in particular the Department of the Lands and Survey and the Department of Fisheries. In particular the authors would like to thank Faatasi Malologa and Dolores Leneuoto, for their support in the lead to and during visits in Tuvalu along with Sam Finikasu, Elemea, Arne Talia, Paeniu Lopati, Semese Alefaio.

Executive summary

Understanding the wave climate changes in the Pacific region is critical for coastal management and to the implementation of climate change adaptation. However, little is known about waves and how reef hydrodynamics is affecting the reef coast of Pacific islands. The Changing Waves and Coast in the Pacific (WACOP) project is collecting baseline information and using the latest research tools to assess the wave climate, its variability, improve the understanding of reef hydrodynamics and morphology as well as predict how these will change with the climate. The project aim is to better understand coastal erosion and inundations and to assess the potential for wave energy harvesting.

The data presented in this document analyses the oceanographic and topographic data recorded during the WACOP project on Fatato Island in Funafuti, Tuvalu. The data shows that the hydrodynamics of the fringing reef in Fatato is controlled by both short waves and infragravity waves, both modulated by the tide. The data presented in this document has been used to calibrate and validate a coastal inundation model that was used to simulate how wave inundation hazard will increase with sea level rise (Beetham et al. 2015).

1 Background

The Pacific island countries (PICs) are vulnerable to climate change, and have a high dependence on imported fossil fuels. Both of these problems can be attributed to the smallness and geographic isolation of PICs. In terms of climate change, a specific disadvantage that arises from the smallness of the islands is a greater coastline to land-area ratio. The majority of urban areas are located in dynamic coastal zones, and, with a total population of 10 million, these tend to be densely populated with a relatively high concentration of infrastructure. The shorelines of PICs are therefore vulnerable areas with the greatest risk of displacement and loss of livelihood assets through erosion and inundation.

These coastal hazards are projected to become more frequent and intense with climate change. However, current coastal vulnerability and adaptation assessments still focus mainly on sea-level rise, with less attention paid to other important coastal change drivers such as ocean surface waves. Waves wear away land and remove beach sediments, and are also a cause of coastal flooding and habitat destruction during extreme events. Wave research is very limited in the PICs, particularly given their dependence on the coast. The limiting factor in assessing the effects of climate change on coastal areas is therefore insufficient information on the variability and trends of ocean waves as a driver of shoreline changes at relevant island and community scales.

PICs lag behind in research about wave climate variability and trends. Only a few short-term (years) *in-situ* wave observations exist, and there have only been a limited number of studies that analyse historical wave climate data in terms of coastal impacts and wave power availability. PICs do not currently conduct research into how wave climate, wave power, and shorelines may evolve under emission scenarios. The poor understanding on how damaging waves, eroding shorelines and wave power have changed in the recent past and how they may change in the future under climate change is a major knowledge gap which will be addressed by the WACOP project.

1.1 Aims of the WACOP project

The project addressed these knowledge gaps in two ways. Firstly, in terms of ocean waves, the project used computer models to downscale public domain data on the historical (decadal) wave variability and trends to relevant regional and local scales, and estimate how wave climate will change in the future under projected climate change scenarios. Secondly, in terms of coastal erosion and inundation, field visits were conducted and data collected at specific local sites to calibrate and validate models (at scales of 10s of metres) that can predict shoreline behaviour under climate change and thereby assist with adaptation and disaster risk reduction. This latter part presents a specific problem as available models have been developed for the open sandy coasts found on continental shorelines. The majority of PIC coasts however are fringed by coral reefs, and adapting existing predictive models to reef environments will involve relevant and original research through this project.

1.2 This report

The field investigations presented in this report were aimed at gathering baseline information on the oceanography of the fringing reef and the beach fronting the shoreline in Fatato, on Funafuti, Tuvalu. This information is critical to better understand the role of waves in coastal hazards (erosion

and inundation) in the Pacific. Fatato is one of 2 sites selected as the Project field sites. A similar report has been produced for the Fringing reef of Maui Bay on the Coral Coast of Fiji (Figure 1).

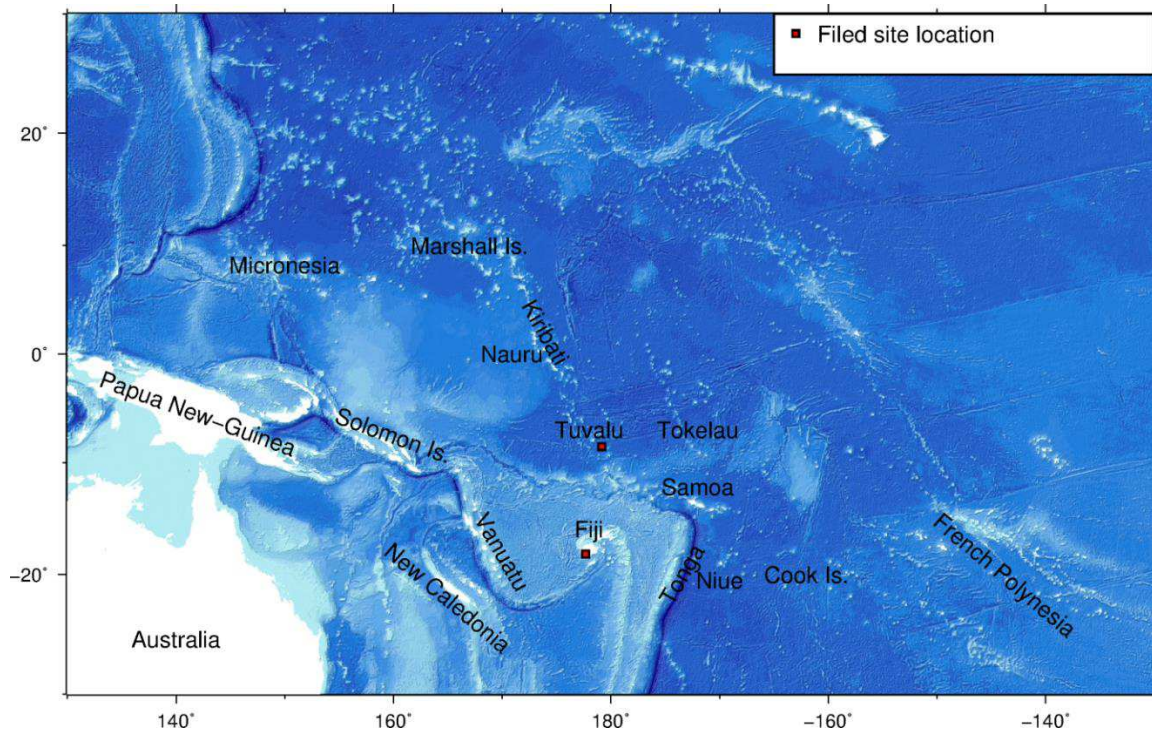


Figure 1.1 WACOP field sites in the Pacific

2 Site Overview

Fatato is one of the 24 islets located on the rim of the atoll of Funafuti in Tuvalu (Figure 2.1). The island of Fatato is the location of the only remaining benchmark from 8 transects aimed at monitoring the evolution of the storm beach formed on the eastern side of Funafuti after the passage of Tropical Cyclone Bebe (Baines and McLean 1976). The profile is important as it constitute one of the longest beach monitoring sites in the Pacific.

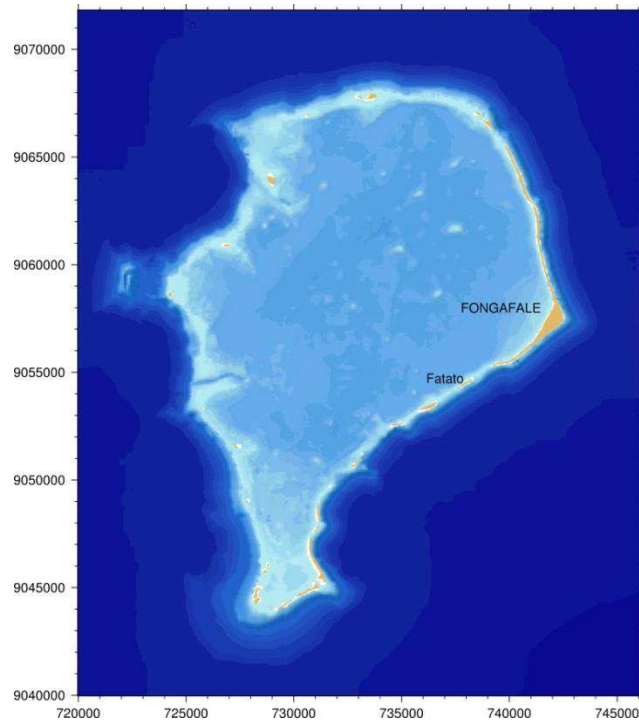


Figure 2.1 Funafuti atoll and the location of Fatato Islet.

2.1 Morphology and Geology

2.1.1 Geography

Fatato Island (Figure 2.2) is a vegetated island 900m long and 100m wide located approximately 1km south of Fongafale southern tip. The Ocean facing shoreline of the island is located approximately 100m from the reef crest. The beach on the ocean side is composed of a mix of sand, pebbles, cobbles, and boulders, with the cobbles size range dominating and forming steep imbricated cobble ridges. The foot of the beach is perched on a cemented beachrock and boulder lag that extend roughly 50m on the reef flat towards the ocean. While part of this cemented lag deposit is clearly linked with the rubble rampart formed during Tropical Cyclone Bebe (Maragos et al. 1973), this layer is likely to have existed prior to this event.



Figure 2.2 Aerial view of Fatato Island taken in January 2013. (Photo: Paul Kench)

2.1.2 Reef flat morphology

Within approximately 50m from the shoreline, the reef flat is laid with a cemented lag deposit (Figure 2.3). The lag deposit is composed of large (>1m diameter) to small boulders cemented with cobbles and coarse sand. The lag deposit shows a weak imbrication and a weak preferential orientation towards both end of the island. The elevation of the lag is highly variable but mostly intertidal, forming pools at low tide. The Ocean edge of the lag is clearly marked but varies greatly alongshore. The offshore side of the reef flat is a smooth, horizontal platform sprinkled with large boulders. Toward the reef crest, acropora colonies are present with an increasing density towards the reef crest. At the crest, the reef is cut with deep grooves, each groove is laid with well-rounded coral boulders (Figure 2.4).



Figure 2.3 Lag deposit on the reef flat in Fatato.

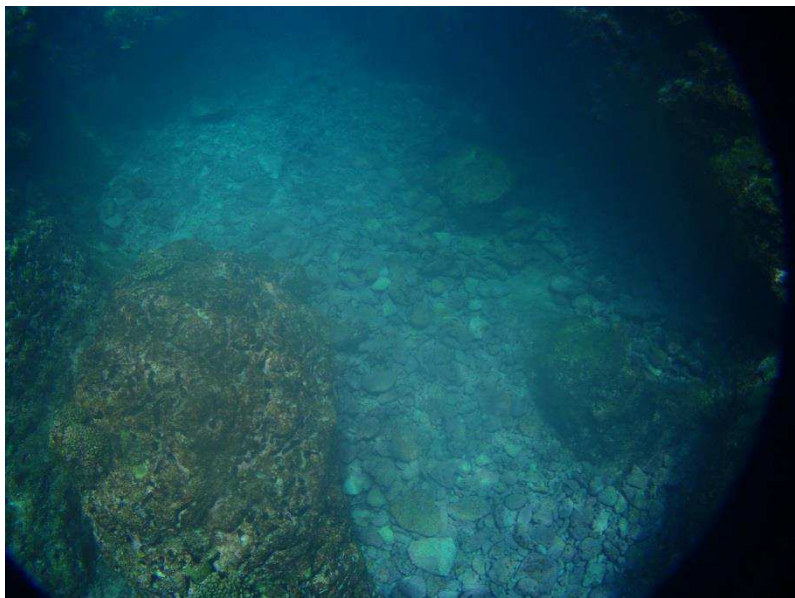


Figure 2.4 Boulder accumulations at the bottom of the grooves near the reef crest at Fatato.

2.1.3 Beach morphology

The beach face in Fatato is steep with near vertical slope near the beach ridge. The steepness of the beach ridge face is made possible by the imbrication of flat-ish rounded coral cobbles and boulders that have likely been created by the dismantlement of coral plates. The beach displays features that are similar to beach cusps, the centre of the cusps often shows an inverse sorting with larger boulders in the upper face of the beach, medium to small cobbles in the middle part and foot of the beach, the sides of the cusps shows a normal sorting (Figure 2.5). Coarse to medium sand can be found filling small cavities on the supratidal reef flat.



Figure 2.5. Normal beach sorting at the south end of Fatato

3 Oceanography

A series of instruments were deployed near Fatato between March 2013 and March 2014 with the aim of measuring the local waves, currents, water level and water temperature across the reef from the offshore reef slope to the shore.

3.1 Deployments

Four oceanographic instruments were deployed along a cross-shore profile (Figure 3.1 and 3.2). A RBR-TWR pressure sensor was installed near the shore (Figure 3.3), an Aquadopp current profiler was installed in the centre of the Reef flat (Figure 3.4), a RBR-TWR pressure sensor was installed near the reef crest (Figure 3.5) and a AWAC current profiler was installed in the reef slope at approximately 20m depth, which was later replaced by a Virtuoso pressure sensor. The brand and set up of each instrument is detailed in table 3.1. At the shore, mid reef and reef crest location ,the reef was drilled and a temporary aluminium frame was bolted to the reef. This allowed for a consistent position of the instrument across multiple deployments and a secure mooring. The reef slope instrument was installed on the reef using a weighted aluminium frame. The frame was deployed and recovered with the instrument and redeployed at the same location each time.



Figure 3.3 RBR-TWR deployed near the shore in Fatato



Figure 3.4 Aquadopp deployed near the centre of the reef flat in Fatato



Figure 3.5 RBR-TWR deployed near the reef crest in Fatato



Figure 3.6 AWAC deployed on the reef slope of Fatato in 20m depth

Table 3.1

| Brand - Instruments name | Location | Time between wave burst (s) | Wave burst duration (s) | Water level /currents ensemble averaging (s) | Interval between water level/currents ensembles (s) |
|--------------------------|------------|-----------------------------|-------------------------|--|---|
| RBR-TWR | Shore | 10800 | 2048 | 240 | 600 |
| Nortek - Aquadopp | Mid-reef | 10800 | 2048 | 120 | 600 |
| RBR-TWR | Reef Crest | 10800 | 2048 | 240 | 600 |
| Nortek - AWAC | Reef slope | 10800 | 2048 | 60 | 600 |

The deployment schedule used was designed to optimise the length of deployment hence, instruments were swapped to limit data gaps between deployments. Some data gaps are unavoidable when instruments break down or batteries die out. A detail of the final schedule is presented in figure 3.7.

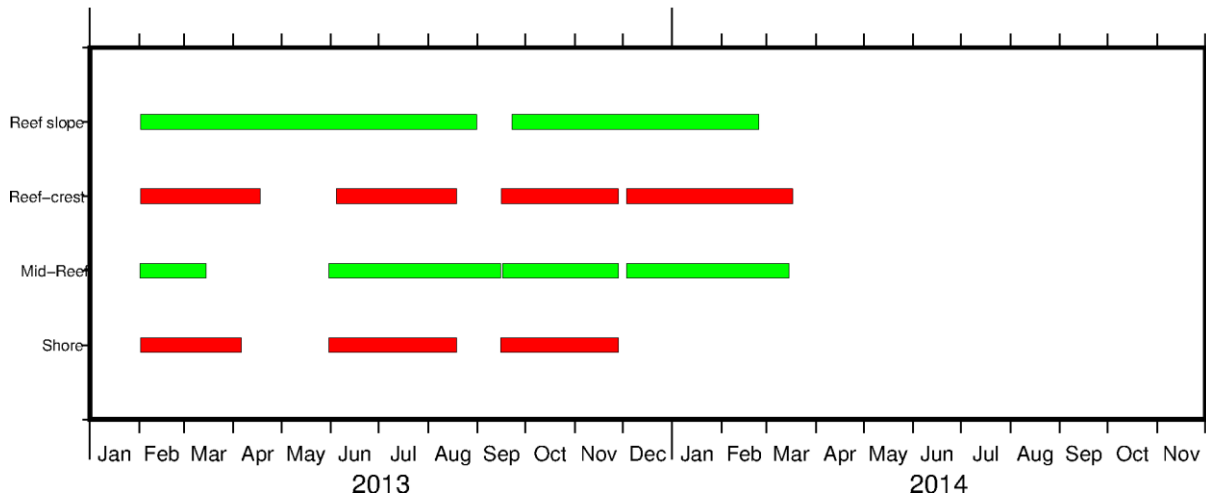


Figure 3.7 Oceanographic deployment schedules for each location in Fatato. This figure shows only the usable collected data.

3.2 Oceanographic data Post processing

The collected data was processed in a consistent way to allow comparison between locations.

3.2.1 Waves

All wave data was collected in burst of pressure data at 1Hz. This data was processed by calculating the power spectrum of the detrended pressure measurements for each data burst using a one-side periodogram. For offshore sites each data burst was corrected to account for pressure damping due to the depth of the instrument. Based on the power spectrum of each burst, the significant wave height (H_s), and infragravity wave height (H_i) was calculated as follow:

$$H_s = 4 \sqrt{\int_{0.05}^{0.3} S df}$$

$$H_i = 4 \sqrt{\int_{0.001}^{0.05} S df}$$

where S is the power spectrum and f is wave frequency.

Similarly, the mean wave period and the infragravity wave period were calculated using the following equations:

$$T_{ms} = \frac{\int_{0.05}^{0.3} S df}{\int_{0.05}^{0.3} S \cdot f df}$$

$$T_{mi} = \frac{\int_{0.001}^{0.05} S df}{\int_{0.001}^{0.05} S \cdot f df}$$

For each burst the wave energy flux (E) was also calculated as:

$$E = \rho g S C g$$

where ρ is the density of water; g is the acceleration due to gravity; and Cg is the wave group velocity which depends on the wave frequency and the depth.

3.2.1.1 Reefslope

The mean wave height of short waves ($T < 20s$) on the reef slope for all the record was 1.05m (Figure 3.8) with a mean wave period of 9.7s (Figure 3.9). For the duration of the record, 5 wave events had a significant wave height higher than 2m and the largest event was 2.49m. The infragravity wave heights recorded at the reef slope were much smaller than the short waves with a mean height of 0.06m. The largest infragravity wave height recorded was 0.18m and did not correspond to the largest wave event (Figure 3.10).

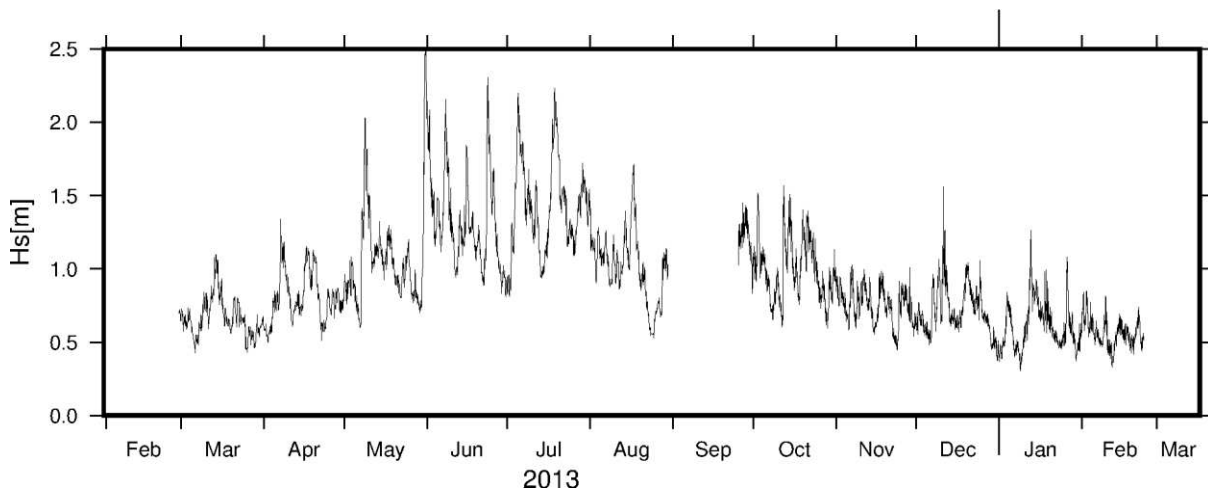


Figure 3.8 Significant wave height recorded on the reef slope

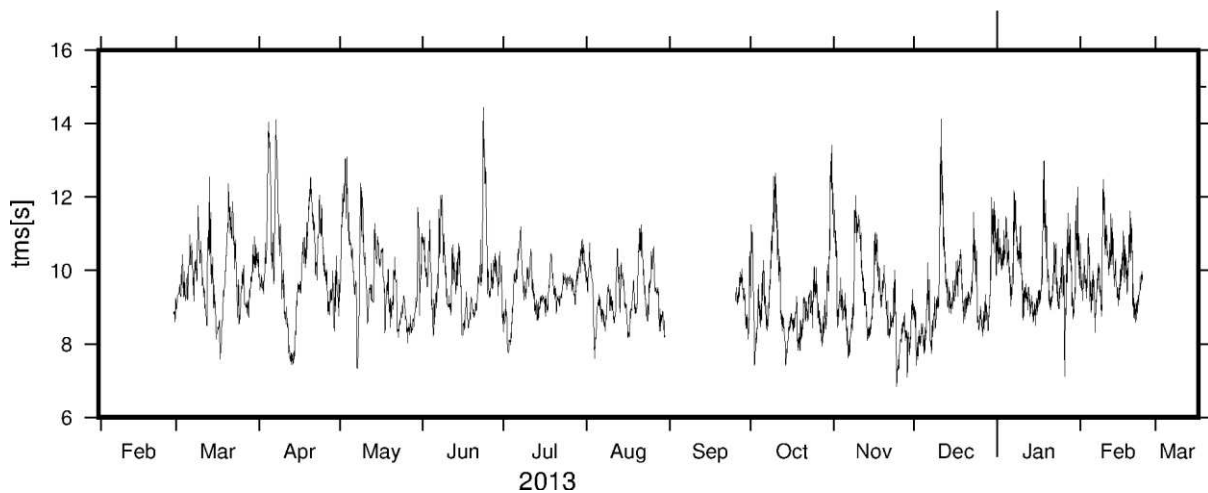


Figure 3.9 Mean wave period of short waves recorded on the reef slope

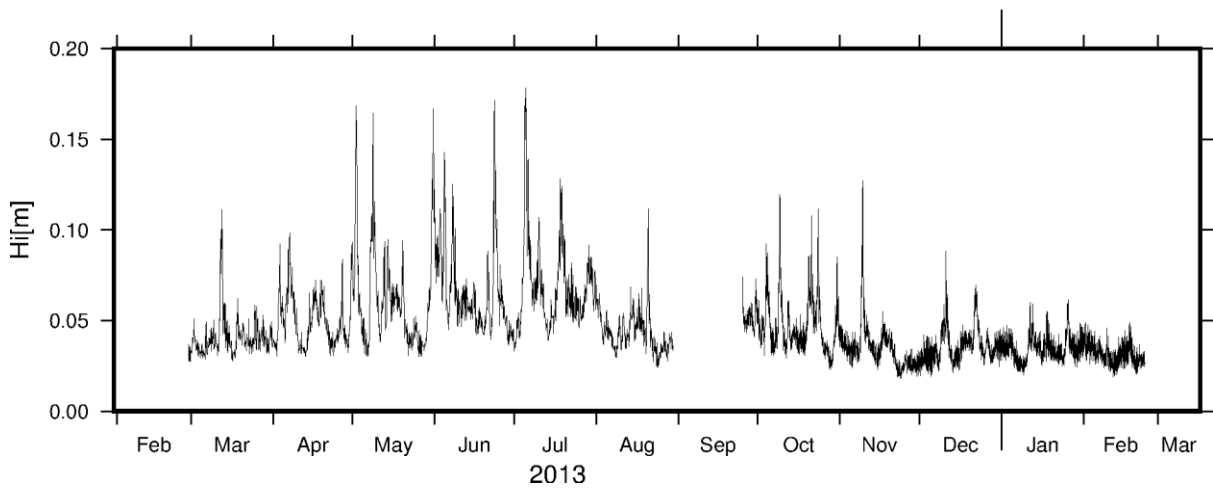


Figure 3.10 Infragravity wave height recorded on the reef slope

3.2.1.2 Reef Crest

Waves on the reef crest were on average smaller than on the reef slope with a mean significant wave height of 0.57m. The waves are also highly modulated by the tide. The largest significant wave height was measured at 1.38m on the 24th of June 2013 (Figure 3.11). The mean wave period (8.2s) was smaller than that of the reef slope site (Figure 3.12).

The infragravity wave height is much larger at the reef crest than on the reef slope with a mean of 0.18m and a maximum of 0.77m during the event that recorded the largest significant wave height (Figure 3.13).

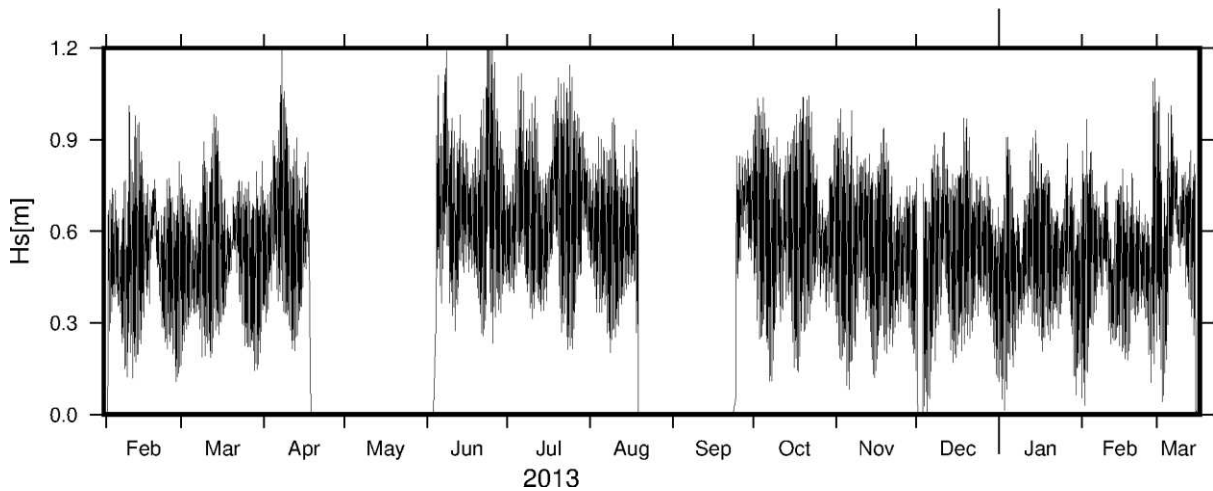


Figure 3.11 Significant wave height recorded on the reef crest

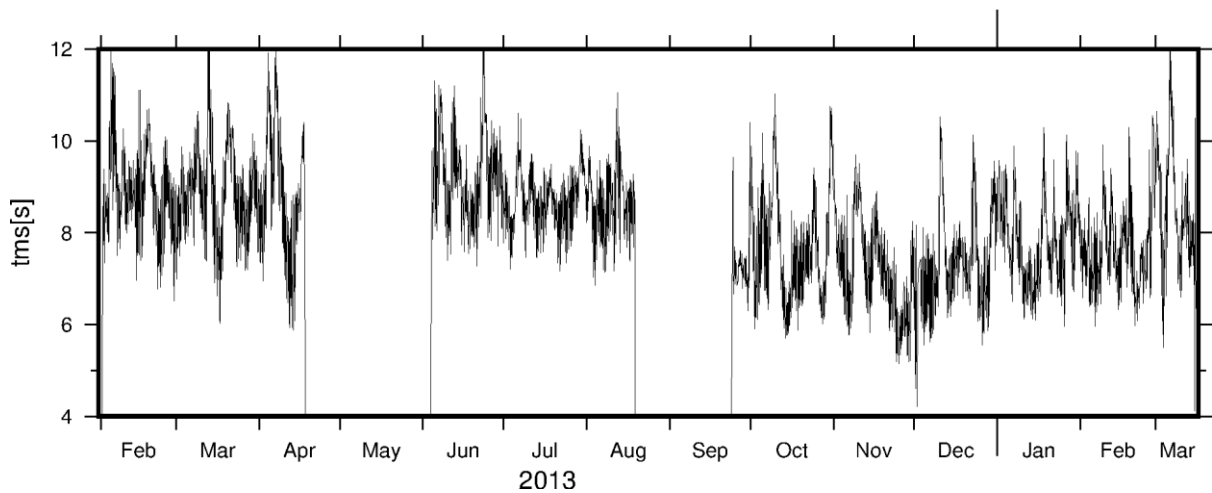


Figure 3.12 Mean wave period of short waves recorded on the reef crest

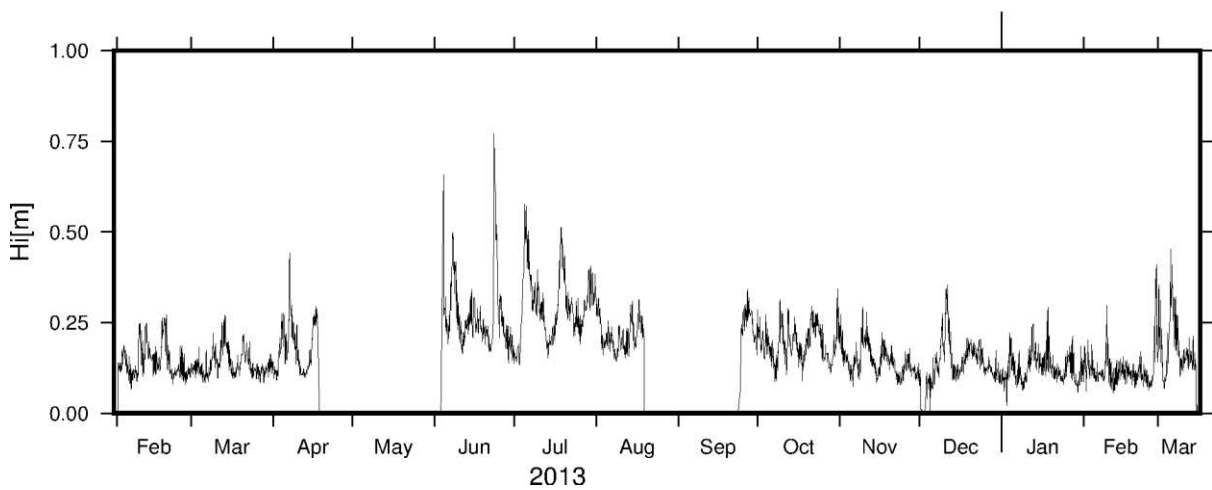


Figure 3.13 Infragravity wave height recorded on the reef crest

3.2.1.3 Shore

Waves recorded at the shore were similar yet smaller than the waves recorded on the reef crest. The mean significant wave height was 0.27m at 8.2s (Figure 3.14, 3.15). Infragravity waves dominate the shores with a mean infragravity wave height of 0.26m (Figure 3.16). The largest infragravity waves were recorded on the 23rd of June 2013 at 0.96m. Similarly to the reef crest the shore location waves are modulated by the tide.

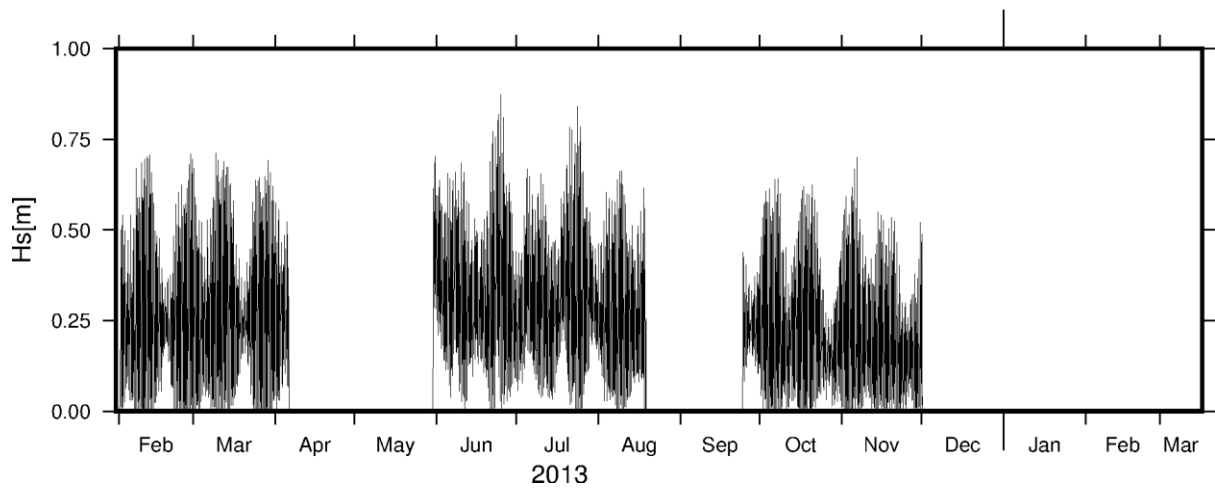


Figure 3.14 Significant wave height recorded on the shore

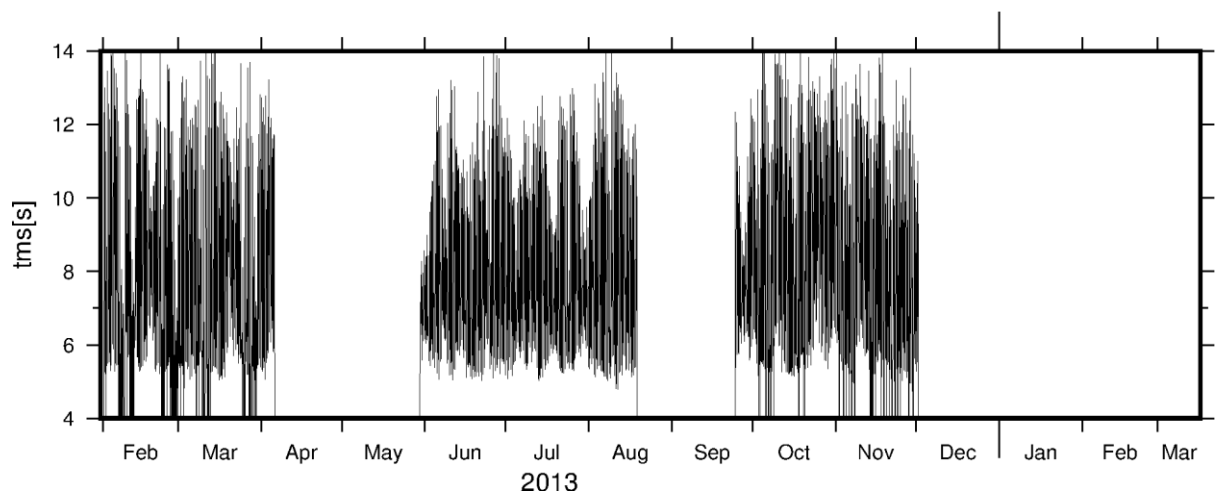


Figure 3.15 Mean wave period of short waves recorded on the shore

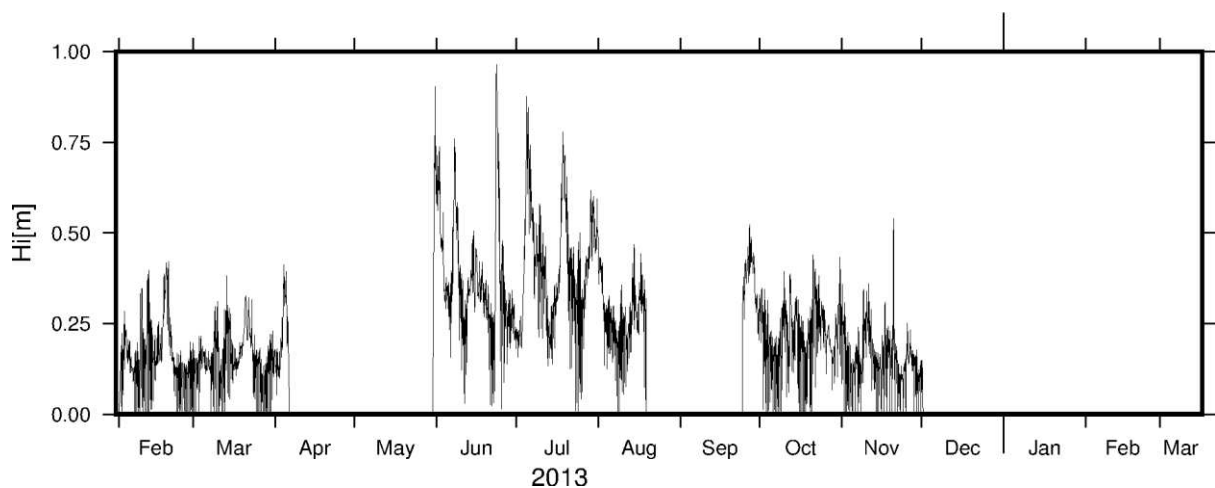


Figure 3.16 Infragravity wave height recorded at the shore

3.2.2 Water levels

The water levels were corrected to reflect the elevation of the water table above Mean Sea Level (hereafter MSL).

3.2.2.1 Reef slope

Water level on the reef slope shows a classic semi-diurnal tide with spring and neap cycles (Figure 3.17). The largest water level was recorded on the 26th of May 2013 at 1.14 m (above mean sea level level). The lowest water level was recorded on the 21st of August 2013 at -1.12m

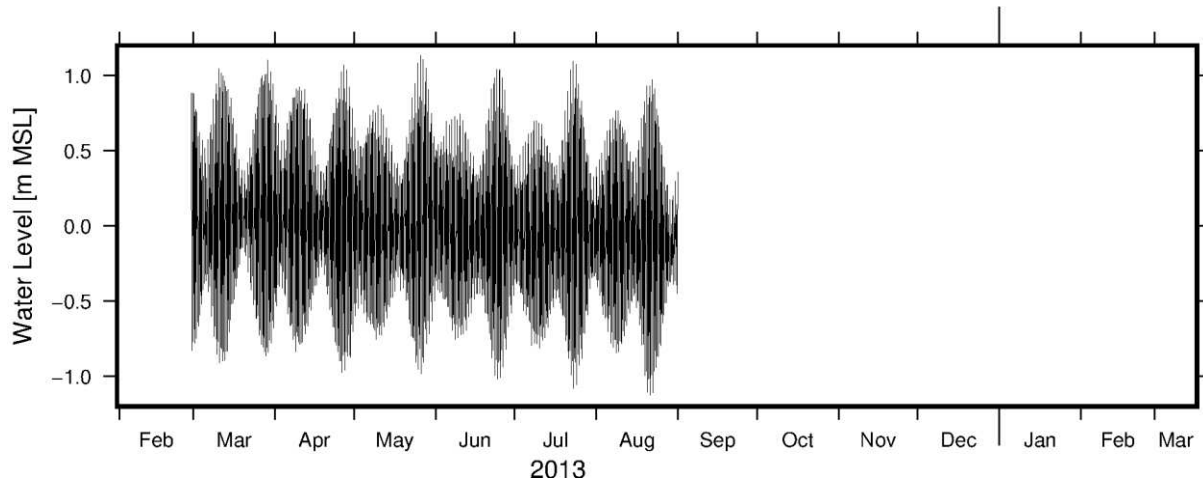


Figure 3.17 Reef slope water levels relative to Mean Sea Level

3.2.2.2 Reef crest

Despite the wave activity, the water level on the reef crest shows a typical semidiurnal signal (Figure 3.18).

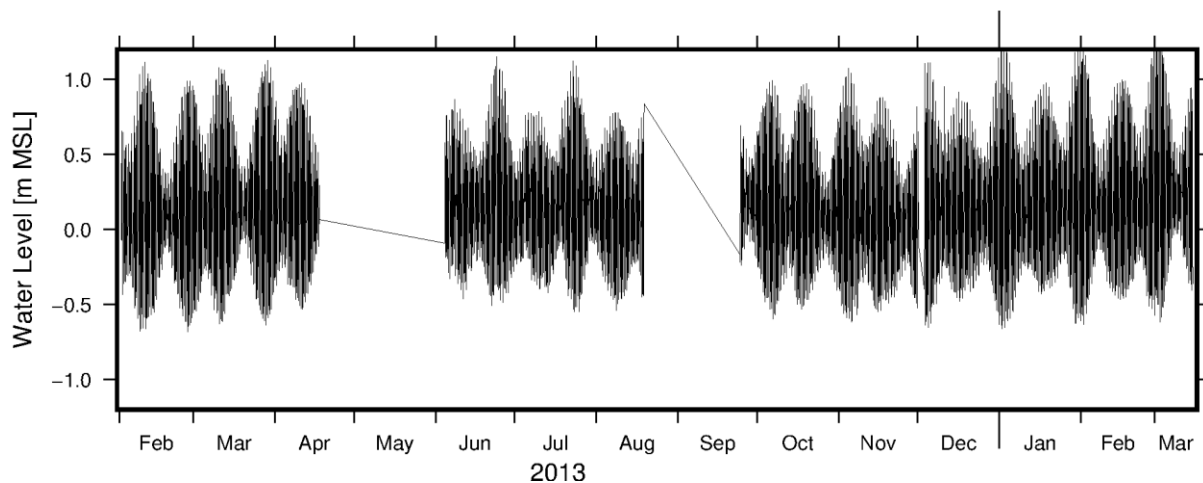


Figure 3.18 Reef crest water levels relative to Mean Sea Level

3.2.2.3 Mid-reef

The signal on the mid-reef is very similar to the reef crest although the instrument emerged at the lowest tides (Figure 3.20)

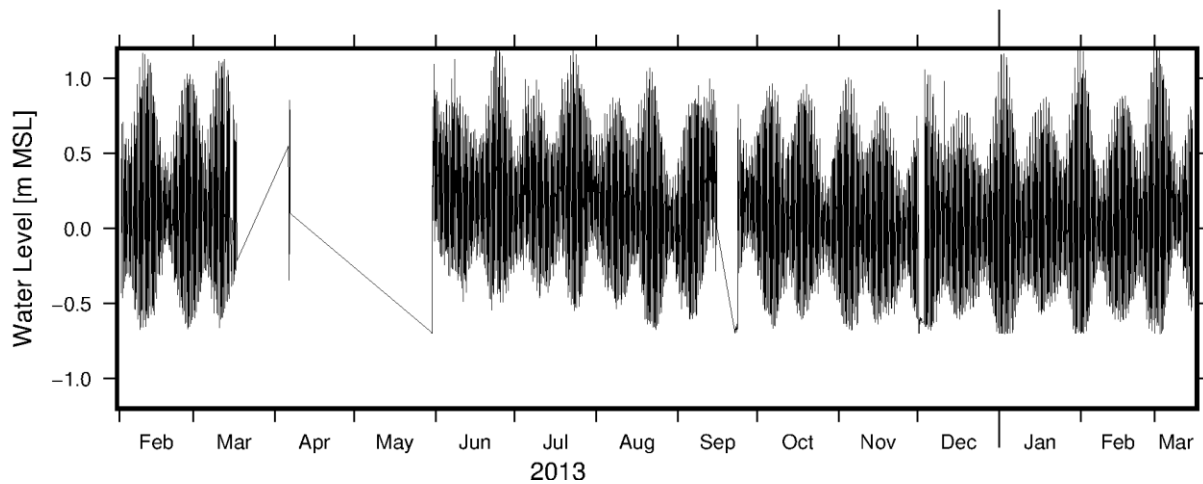


Figure 3.20 Mid-reef water levels relative to Mean Sea Level

3.2.2.4 Shore

Water level at the shore is similar to the mid-reef water level only truncated below -0.2m MSL which is the elevation of the tide pool where the instrument was installed (Figure 3.21).

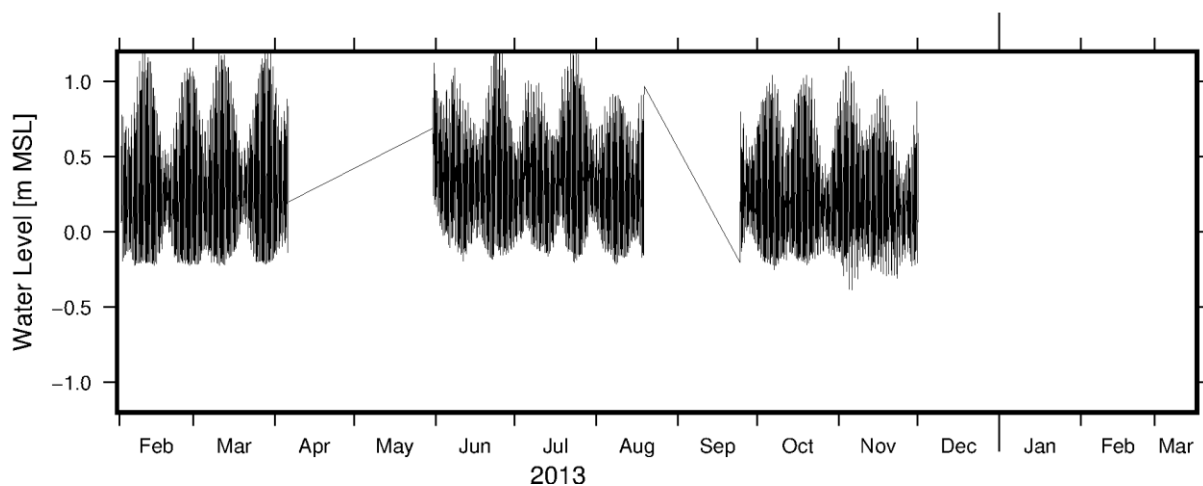


Figure 3.21 Shore water levels relative to Mean Sea Level

3.2.3 Currents

Currents were averaged through the water column and are presented as longshore/crossshore components.

On the reef flat of Fatato the currents are mainly driven by waves and are therefore mostly crossshore. The longshore component shows a tendency towards positive or negative depending of the season (Figure 3.22), this reversal of the current is likely to be driven by the seasonal changes in the dominant wave direction.

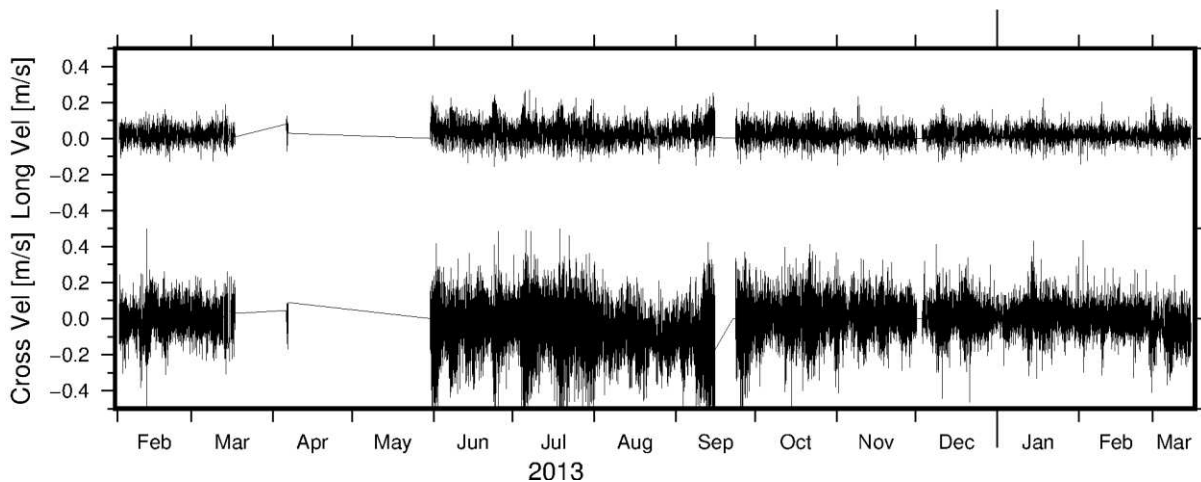


Figure 3.22 Crossshore and longshore component of the current velocity at the mid-reef site in Fatato.

3.2.4 Tide

Tides are evidently an important oceanographic process in Fatato. However the water levels on the reef flat are mostly controlled by waves which are modulated by the tide. To better understand the role of the tide a tidal analysis of the water level was conducted. The tide analysis was completed for the offshore water level using the T-Tide software (Pawlowicz et al. 2002). The form factor (Haigh et al. 2011) was calculated and compared with common ranges (Pugh, 2004).

Tidal analysis provided the amplitude and phase of the principal constituent of the tide (Table 3.2). The tide form factor was calculated as 0.16 which correspond to a semidiurnal form.

Table 3.2 Amplitude of tidal constituents in Fatato extracted from offshore water levels

| Constituent | M2 | S2 | N2 | K1 | K2 | O1 | P1 | SSA |
|---------------|--------|--------|--------|--------|--------|--------|--------|--------|
| Amplitude (m) | 0.5698 | 0.2322 | 0.1432 | 0.0815 | 0.0651 | 0.0514 | 0.0289 | 0.0515 |

3.2.4.1 Exceedance Curve

The Mean High Water Perigean Spring high tide often referred to as “King tides” is the amplitude of the M2, S2 and N2 tidal harmonics, this tidal level (0.95m) (Table 3.3) is exceeded by 8% of high tides. The mean high water spring (Spring high tides) is the combined amplitude of the M2 and S2 tidal harmonics (0.80m), here exceeded by 20% of high tides. The Mean high Water is the mean elevation of all high tide (0.60m) and the Mean High Water neap is the difference in amplitude of the M2 and S2 tidal harmonics level of the tide (0.34m) exceeded by 85% of high tides (Figure 3.23).

Table 3.3 Common tidal elevation for Fatato offshore waters

| | Mean High Water Perigean Spring (MHWPS) | Mean High Water Spring (MHWS) | Mean High Water (MHW) | Mean High Water Neap (MHWN) |
|---------------------------------|---|-------------------------------|-----------------------|-----------------------------|
| Values (m above mean sea level) | 0.9452 | 0.802 | 0.5964 | 0.3376 |

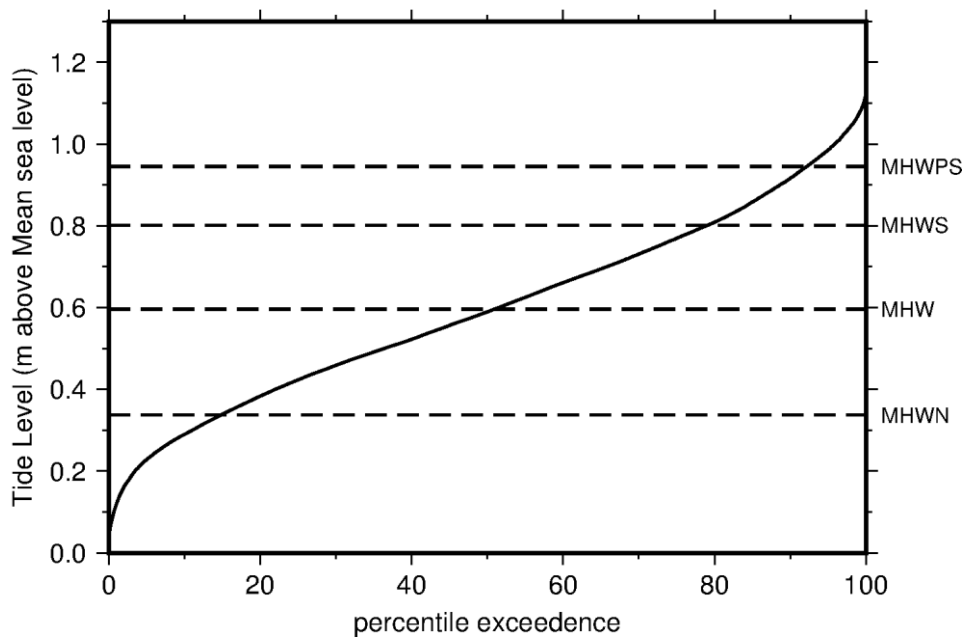


Figure 3.23 Tidal level percentile exceedence curve

4 Topography

4.1 Benchmarks

Benchmarks are essential to create reference points that will allow combining and comparing of all the geographical information collected for Fatato. 12 new benchmarks were placed on the beachrock at Fatato (Table 4.1). The newly installed benchmarks were referenced using a 1h static GNSS survey each of which was corrected using the AUSPOS 2.0 (Geoscience Australia) software. The TAPU benchmark already existed and was re-surveyed using the same method as other benchmarks.

Table 4.1 Benchmark summary, ordered from East to West

| Benchmark name | Longitude | Latitude | Ellipsoid height (m) | Geoid height (m) |
|----------------|------------|-----------|----------------------|------------------|
| FAT1 | 179.165178 | -8.545180 | 36.63 | 1.49 |
| FAT2 | 179.165064 | -8.545984 | 36.66 | 1.52 |
| FAT3 | 179.164530 | -8.546548 | 37.41 | 2.27 |
| FAT4 | 179.163816 | -8.547055 | 37.58 | 2.43 |
| IBM | 179.163135 | -8.547447 | 36.81 | 1.66 |
| PBM | 179.163033 | -8.547516 | 38.04 | 2.89 |
| TAPU | 179.162963 | -8.547549 | 37.68 | 2.52 |
| FAT5 | 179.162189 | -8.548027 | 36.67 | 1.51 |
| FAT6 | 179.161513 | -8.548455 | 36.96 | 1.80 |
| FAT7 | 179.160646 | -8.548937 | 37.96 | 2.79 |
| FAT8 | 179.159949 | -8.549390 | 36.73 | 1.56 |
| FAT9 | 179.159091 | -8.549849 | 36.69 | 1.51 |
| FAT10 | 179.158652 | -8.549938 | 37.31 | 2.13 |

4.2 Beach Profile

Crossshore elevation profiles were collected at each benchmark using total station. The elevation and distance were corrected to reflect the relative elevation of the benchmark and the distance to the benchmark was set to negative shoreward (Figure 4.1 – 4.13).

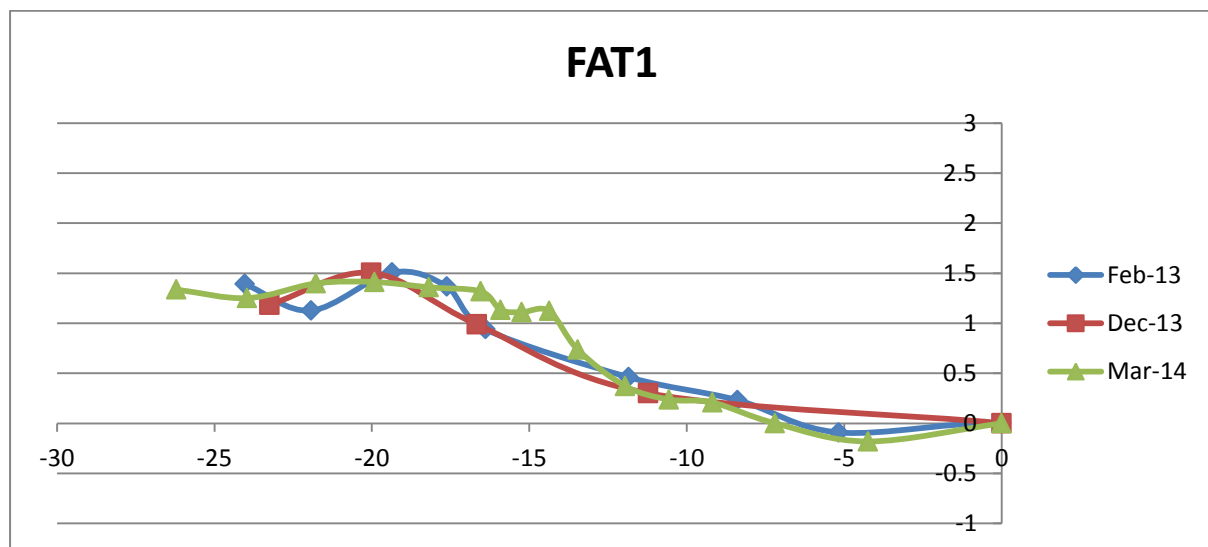


Figure 4.1 Beach elevation profile at benchmark FAT1.

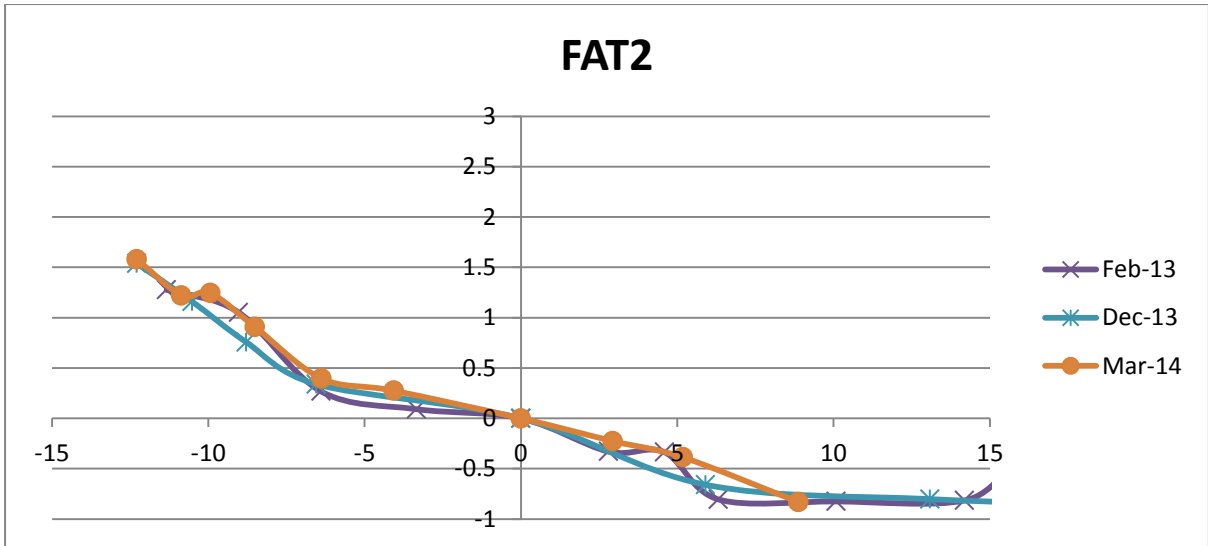


Figure 4.2 Beach elevation profile at benchmark FAT2.

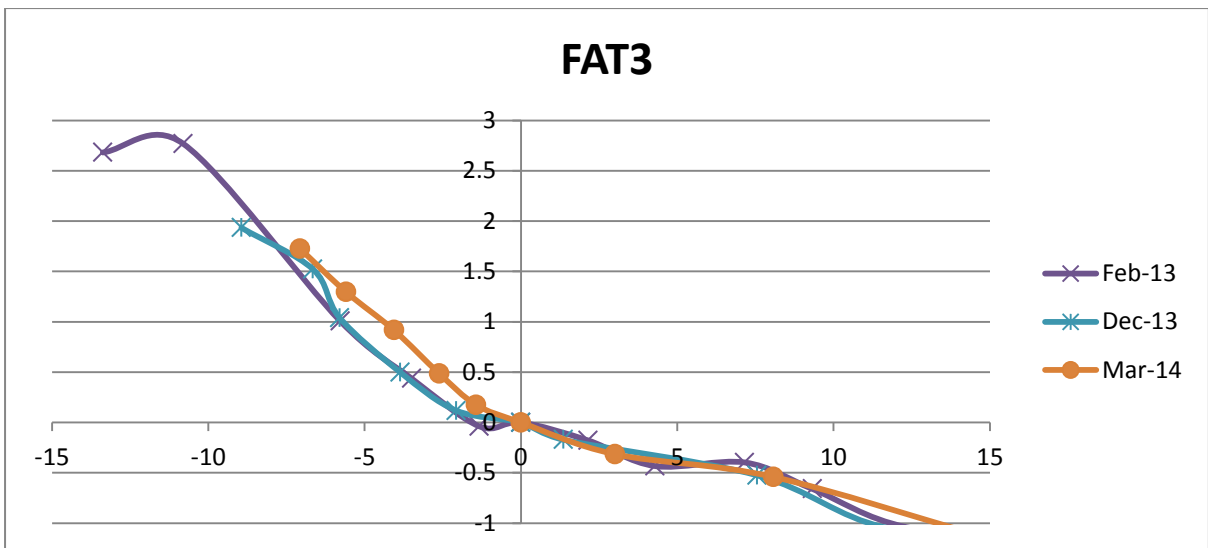


Figure 4.3 Beach elevation profile at benchmark FAT3.

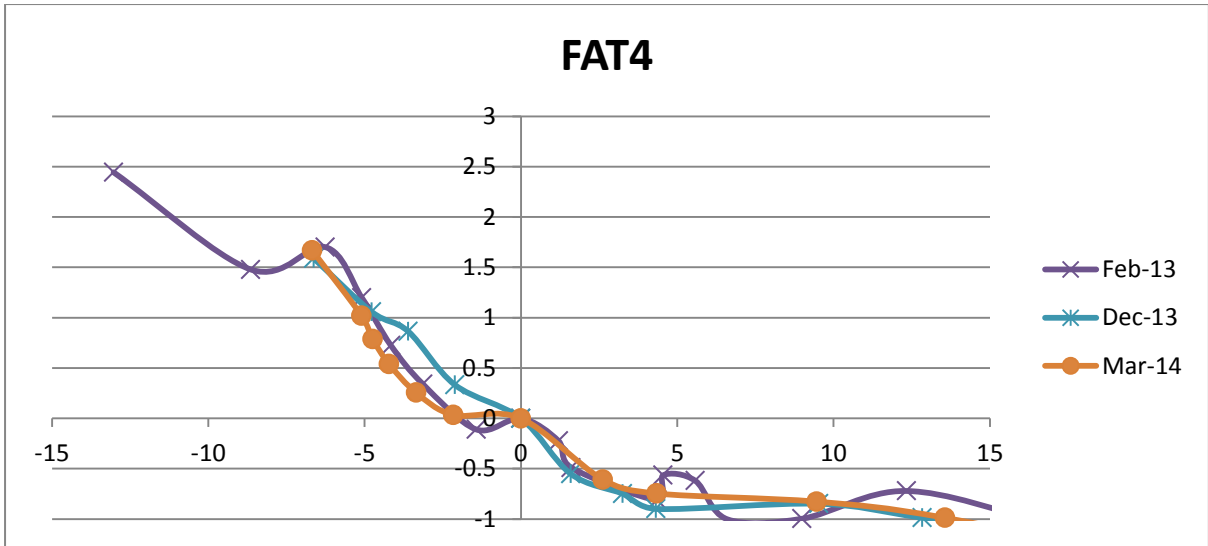


Figure 4.4 Beach elevation profile at benchmark FAT4.

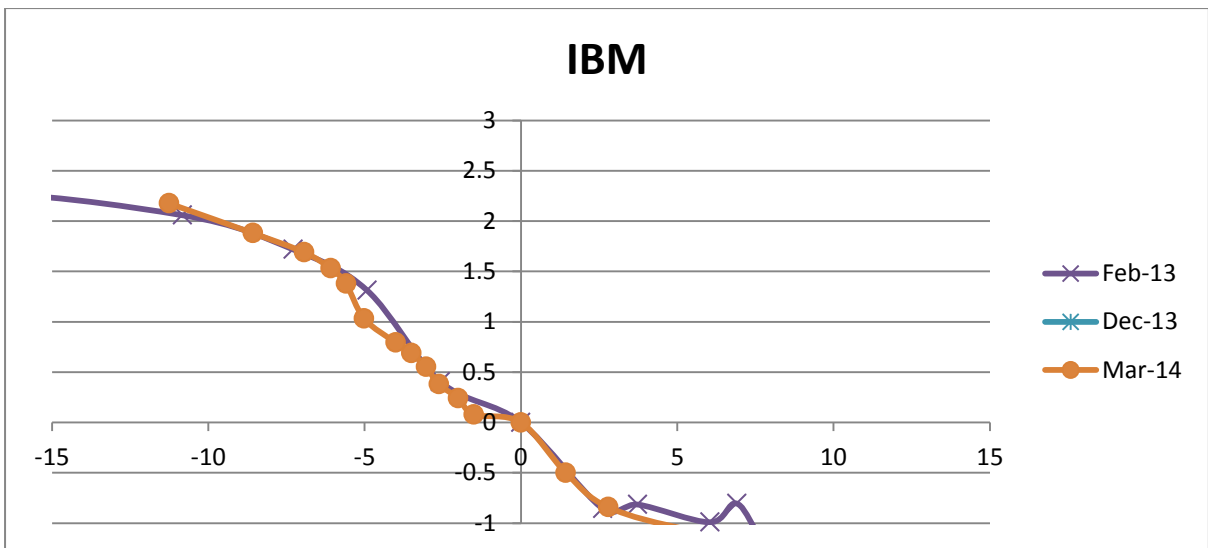


Figure 4.5 Beach elevation profile at benchmark IBM.

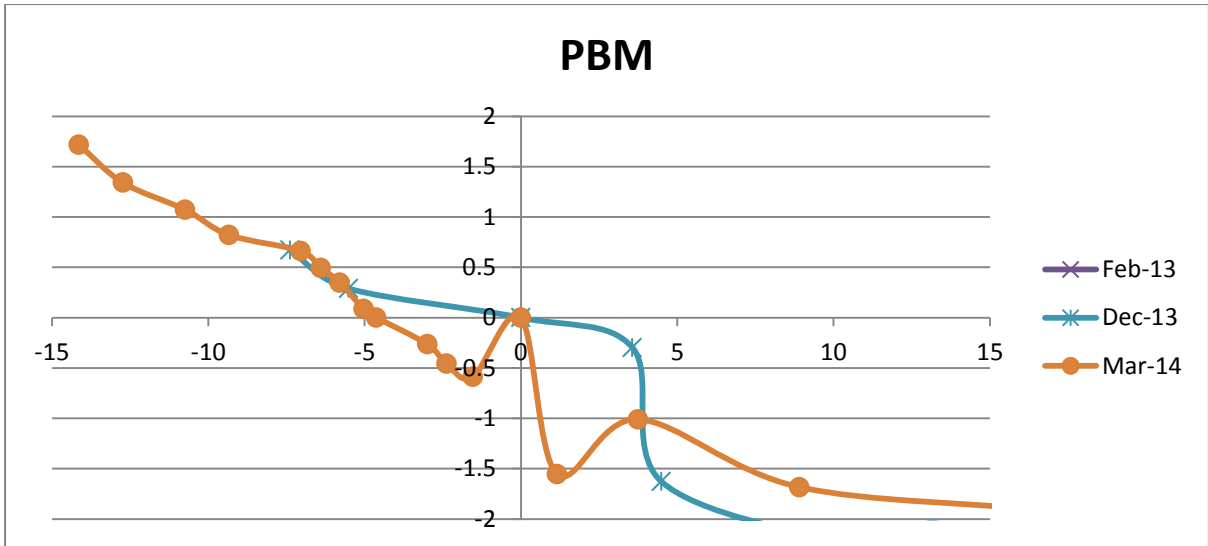


Figure 4.6 Beach elevation profile at benchmark PBM.

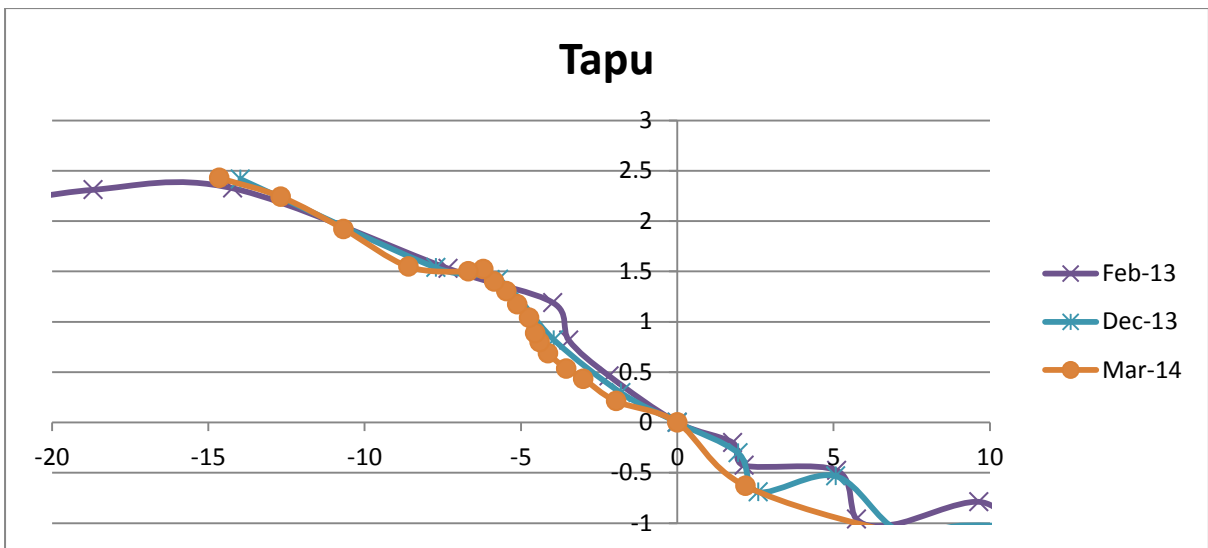


Figure 4.7 Beach elevation profile at benchmark TAPU.

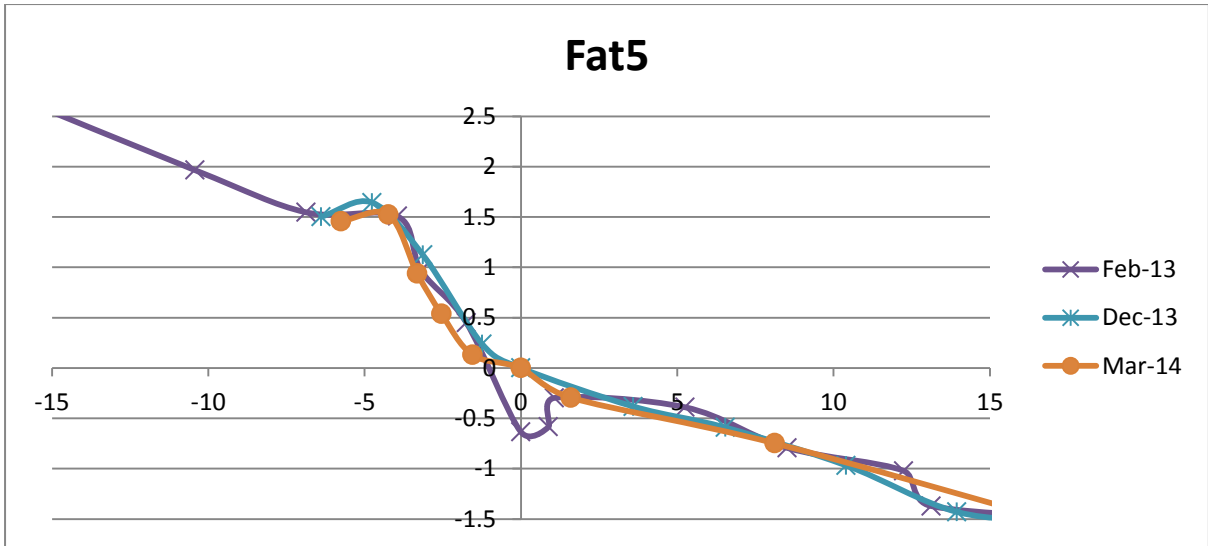


Figure 4.8 Beach elevation profile at benchmark FAT5.

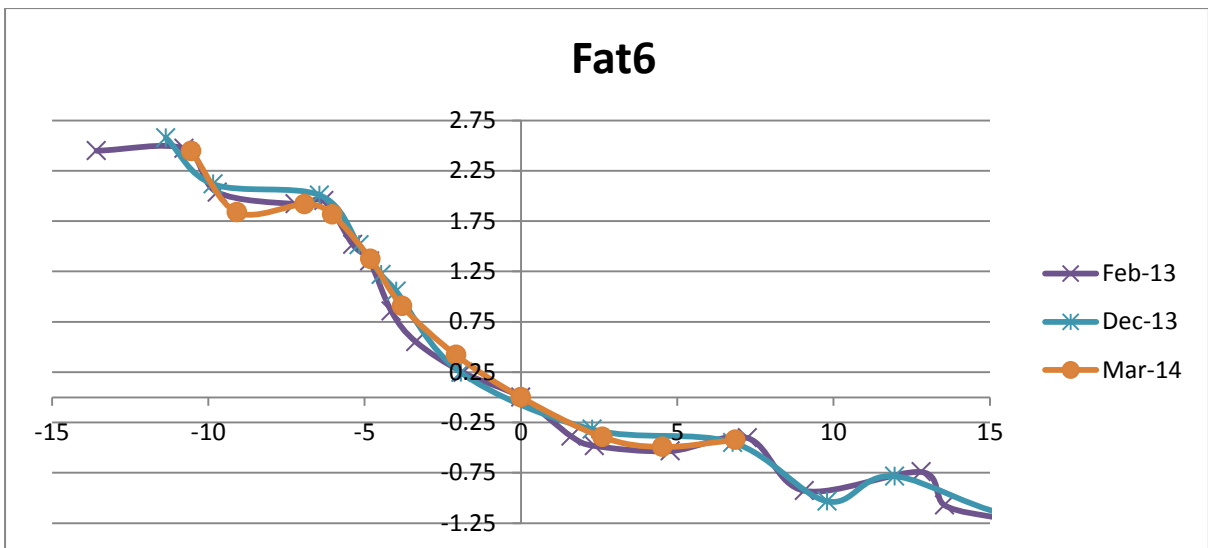


Figure 4.9 Beach elevation profile at benchmark FAT6.

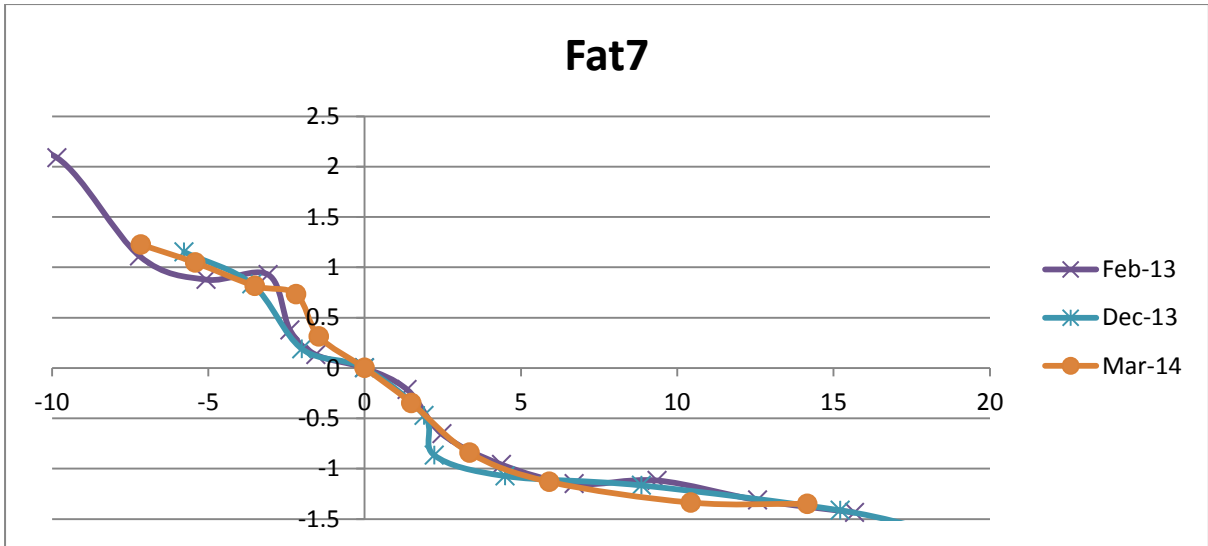


Figure 4.10 Beach elevation profile at benchmark FAT7.

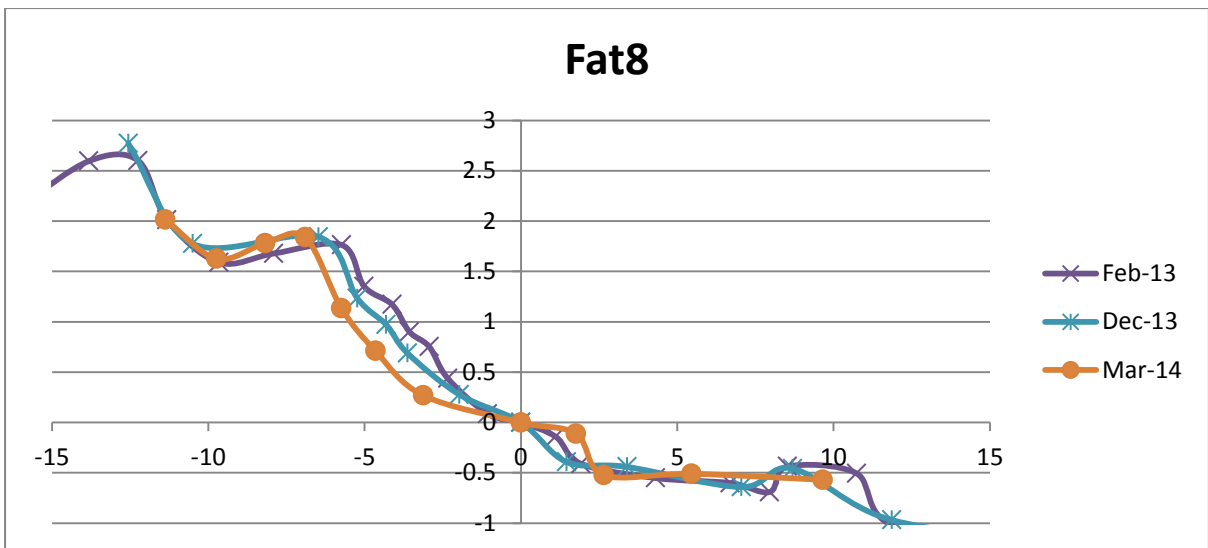


Figure 4.11 Beach elevation profile at benchmark FAT8.

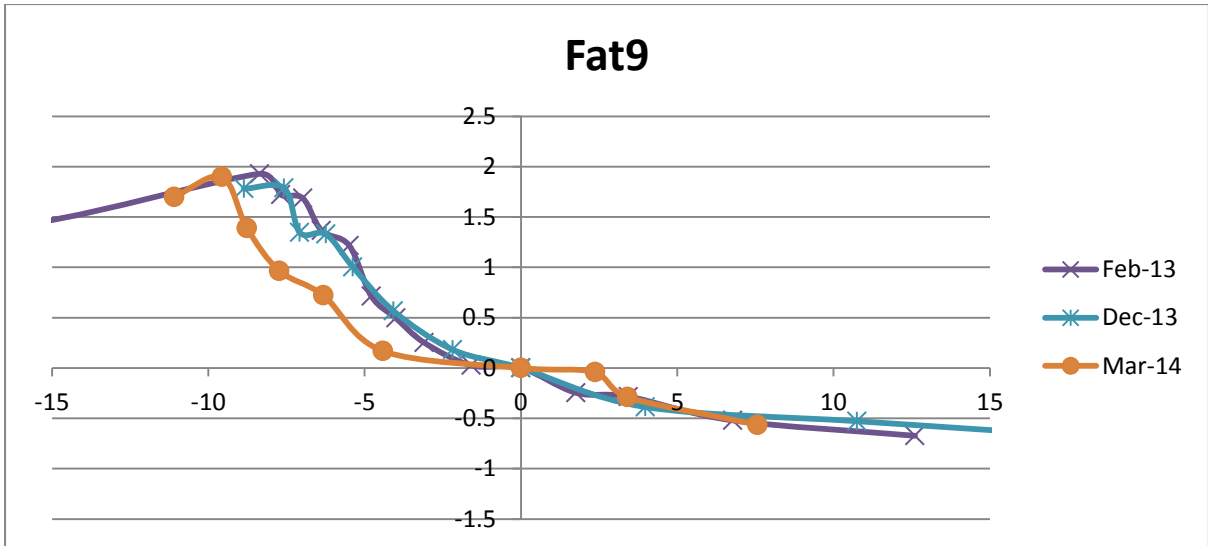


Figure 4.12 Beach elevation profile at benchmark FAT9.

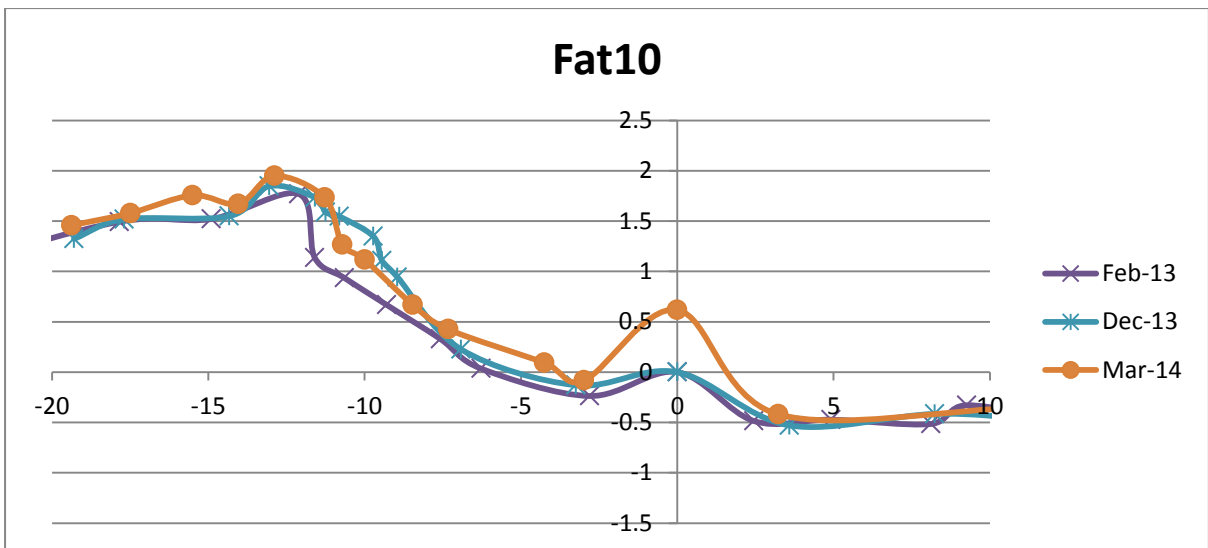


Figure 4.13 Beach elevation profile at benchmark FAT10.

4.3 PPK topography

The topography of the reef flat was measured using a Post Process Kinetic GNSS survey. The GNSS Base station was located at the instrument benchmark and covered a longshore extent between BM3 to BM6 (Figure 4.14)

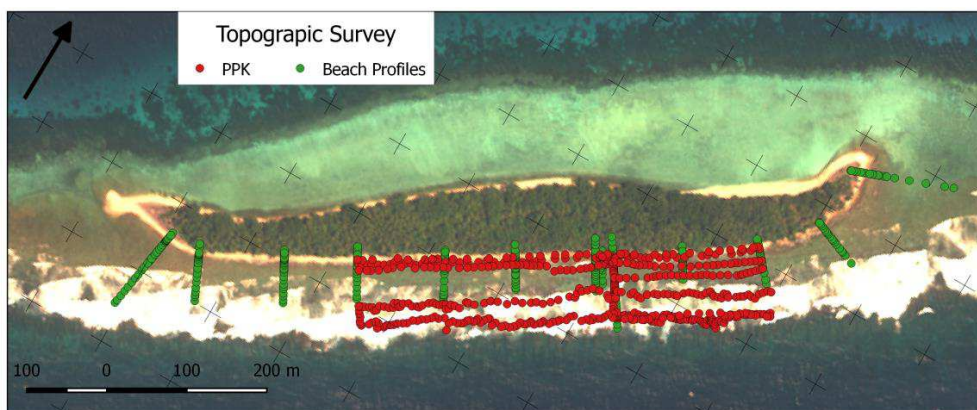


Figure 4.14 Survey extent of the topographic survey of the reef flat in Fatato

5 Shoreline

Historical images were georeferenced against the 2010 IKONOS imagery (Table 5.1), the resulting error is estimated to be less than 4.0m . The toe of the beach (where visible) was used as a proxy for shoreline (Boak and Turner, 2005) and digitized (Figure 5.1) for the whole island, forming a closed polygon. The area covered by each polygon was calculated and the progressive change in the island footprint estimated (Table 5.2).

The digitised shorelines show large changes between 1943 and 1984 with the shoreline on the ocean side prograding 25m, and the area of the island increasing by 15%. By 2002, the shoreline on the ocean side had receded back to the 1945 position and the island had migrated to the South West by 45m (29m in the North East end and 60m in the South West end). From 2002 to 2014 the shoreline on both the lagoon side and the ocean side have shown only small variation (less than 11m of maximum deviation).

Table 5.1 Summary of imagery georeferenced for shoreline analysis

| Imagery date | Type (Source) | Resolution (m) | Georeferencing error estimate (m) |
|--------------|---------------------------------|----------------|-----------------------------------|
| 1943 | Aerial-BW | 0.15 | 3.6 |
| 1984 | Aerial-BW | 0.22 | 2.4 |
| 2002 | Satellite-Colour (Ikonos) | 0.60 | 1.0 |
| 2005 | Satellite-Colour (DigitalGlobe) | 0.75 | 1.5 |
| 2008 | Satellite-Colour (Ikonos) | 0.63 | 2.0 |
| 2010 | Satellite-Colour (Ikonos) | 2.0 | Reference |
| 2012 | Satellite-Colour (DigitalGlobe) | 0.82 | 0.8 |
| 2014 | Satellite-Colour (DigitalGlobe) | 0.82 | 2.1 |

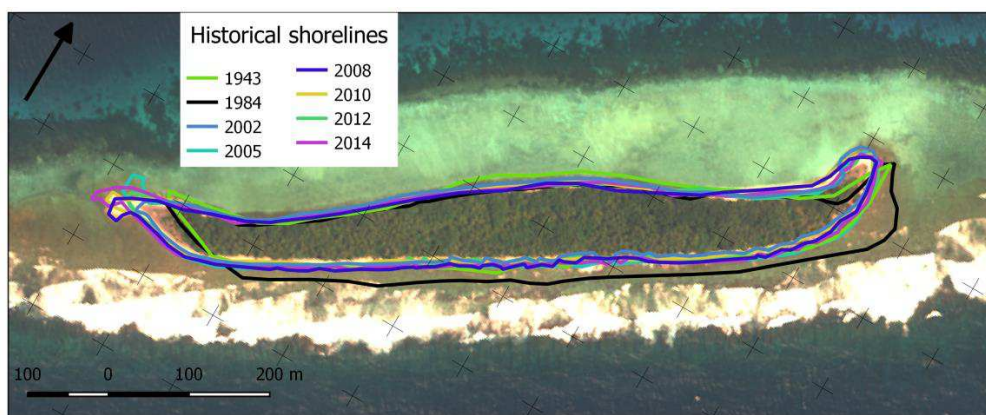


Figure 5.1 Digitized shorelines for Fatato Island

Table 5.2 Summary of Area covered by Fatato Island since 1943

| Imagery date | Area (m ²) | Area changes since 1943 (%) |
|--------------|------------------------|-----------------------------|
| 1943 | 69,620 | 0 |
| 1984 | 79,767 | 15 |
| 2002 | 66,061 | -5 |
| 2005 | 72,232 | 4 |
| 2008 | 69,916 | 0 |
| 2010 | 66,791 | -4 |
| 2012 | 66,313 | -5 |
| 2014 | 71,115 | 2 |

6 Discussion :Fatato Morphodynamics from month, years and decades

The steep beach faces observed in Fatato are composed of imbricated cobble and boulders, suggesting that the beach is often exposed to rough swash conditions. Indeed, the short waves and the infragravity waves at the shore often exceed 0.5m, together the short waves and infragravity are driving a very dynamic swash.

The seasonal change in wave direction is likely to be the driver of coastal drift from North East to South West between September and February and from the South West to the North East between March and August. This seasonal variability is likely to be driving the variability in the morphology of the beach and in the supply of sediment. The coastal drift of sediment is likely to be very variable from year to year because of variability of dominant wave directions driven by a balance between the storm activity in the Southern Ocean which brings South swells and the trade winds which bring Easterly waves. This variability is likely responsible for the changes in shoreline position since 2002 which changes the total footprint of the island by +/-5%. These changes seem to eventually cancel out as the island appears stable over several decades.

The shoreline changes due to extreme events can influence the shoreline position for multiple decades. The huge sediment supply brought to Fatato by Severe Tropical Cyclone Bebe was still obvious 13 years after the event. In less than 30 years after the event the island returned to a

position and shape similar to pre-cyclone. . This hints that the islands present position is a very stable balance between the beachrock footings, the dynamic swash, sediment supply and climate variability. However this stability may be more and more disrupted by the rising sea levels which slowly make the beach face more and more active which should exacerbate the coastal drift.

7 Conclusion

Observation of waves and water level shows that long period infragravity waves dominate the dynamics of the reef system. The dataset presented in this report has been briefly analysed here and can yield far more results pending deeper analysis and numerical modelling.

8 Data download and Citation

The processed data presented in this report may be downloaded on the PacGeo web portal

Wave data offshore

<http://www.pacgeo.org/documents/29685>

Wave data shore

<http://www.pacgeo.org/documents/2966>

Wave data Mid reef

<http://www.pacgeo.org/documents/2967>

Wave data reef crest

<http://www.pacgeo.org/documents/2968>

Waterlevel offshore

<http://www.pacgeo.org/documents/2961>

Waterlevel shore

<http://www.pacgeo.org/documents/2962>

Waterlevel Mid reef

<http://www.pacgeo.org/documents/2963>

Waterlevel reef crest

<http://www.pacgeo.org/documents/2964>

When using the data for publication, please cite this report:

Bosserelle C., Lal D., Movono M., Begg Z., Kumar S., Reddy S., Beetham E., Pohler S., Kench P., Krüger J. Fatato (Tuvalu), Oceanographic, Topographic Data Collection, SPC technical report SPC00045, 2016

9 Reference

Baines, G. B. K., & Mclean, R. F. (1976). Sequential studies of hurricane deposit evolution at Funafuti atoll. *Marine Geology*, 21, 1–8.

Beetham, E., P. S. Kench, J. O'Callaghan, and S. Popinet (2016), Wave transformation and shoreline water level on Funafuti Atoll, Tuvalu, *J. Geophys. Res. Oceans*, 121, 311–326, doi:10.1002/2015JC011246.

Haigh, I. D., Eliot, M., & Pattiaratchi, C. (2011). Global influences of the 18.61 year nodal cycle and 8.85 year cycle of lunar perigee on high tidal levels. *Journal of Geophysical Research*, 116(C6), C06025. doi:10.1029/2010JC006645

Maragos, J. E., Baines, G. B. K., & Beveridge, P. J. (1973). Tropical Cyclone Bebe Creates a New Land Formation on Funafuti Atoll. *Science*, 181(4105), 1161–1164.

Geoscience Australia, <http://www.ga.gov.au/scientific-topics/positioning-navigation/geodesy/auspos>

Pawlowicz, R., Beardsley, B., and Lentz, S. (2002), Classical tidal harmonic analysis including error estimates in MATLAB using T_TIDE, *Computers and Geosciences* 28, 929-937.

Pugh, D. T. (2004), *Changing Sea Levels: Effects of Tides, Weather and Climate*, 280 pp., Cambridge Univ. Press, Cambridge, U. K.



CONTACT DETAILS
Pacific Community

SPC Headquarters
BP D5,
98848 Noumea Cedex,
New Caledonia
Telephone: +687 26 20 00
Fax: +687 26 38 18

SPC Suva Regional Office
Private Mail Bag,
Suva,
Fiji,
Telephone: +679 337 0733
Fax: +679 337 0021

SPC Pohnpei Regional Office
PO Box Q,
Kolonia, Pohnpei, 96941 FM,
Federated States of Micronesia
Telephone: +691 3207 523
Fax: +691 3202 725

SPC Solomon Islands
Country Office
PO Box 1468
Honiara, Solomon Islands
Telephone: +677 25543 /
+677 25574
Fax: +677 25547

Email: spc@spc.int
Website: www.spc.int